OBSERVATIONS AND IMPLICATIONS OF NATURAL LAMINAR FLOW ON PRACTICAL AIRPLANE SURFACES

ICAS-82-5.1.1

B. J. Holmes*
NASA Langley Research Center
Hampton, Virginia 23665

C. J. Obara**
Kentron Technical Center
Division of LTV
Hampton, Virginia 23665

Abstract

Recent flight experiment observations have recorded extensive regions of natural laminar flow (NLF) boundary layers in the favorable pressure gradient regions on several smooth, production-quality airframes. These observations have resulted in a new appreciation of the operational practicality for obtaining NLF on certain modern practical airplane surfaces. The flight experiments were conducted on eight different airplanes, including both propeller- and turbojet-powered configurations and airframes constructed of aluminum or composites. The experiments were conducted on surfaces which received (with two noted exceptions) no special preparation of contours or surface waviness for NLF considerations. Experimentally observed laminar flow transition Reynolds numbers ranged between 1 and 5 million on the propeller-driven airplanes and exceeded 11 million on the business jet tested.

The summarized results of these experiments include comparisons between measured and empirically predicted allowable surface waviness, comparison of flight-measured wing profile drag with tunnel data, comparisons of fixed and free transition airfoil and airplane aerodynamics, and comparisons between observed sweep effects on laminar flow and an empirical spanwise contamination criterion. Also discussed are the observations of laminar flow in the propeller slipstreams of two airplanes, and an example of insect debris contamination on an NLF wing. Several implications of these observations are also discussed, including the necessity for both fixed and free transition flight testing on airplanes with surfaces smooth enough for laminar flow.

Nomenclature

b	wing span, ft
c	airfoil chord, ft
c_ℓ	section lift coefficient
C_L	trimmed airplane lift coefficient, $(W/S)/q_\infty$
C_d	section drag coefficient
C_p	pressure coefficient, $(p_\ell - p_\infty)/q_\infty$
D	propeller diameter, ft
h	density altitude, ft MSL
J	advance ratio, V/nD
M	free-stream Mach number
n	propeller rotation, revolutions per minute
p	static pressure, lb/ft^2
q	dynamic pressure, lb/ft^2
r	leading-edge radius, in.
R_c	Reynolds number based on free-stream conditions and local airfoil chord
R_t	Reynolds number based on free-stream conditions and longitudinal length to transition
R_x	unit Reynolds number based on free-stream conditions
R_θ	attachment line boundary-layer momentum thickness Reynolds number based on free-stream conditions and leading-edge radius normal to the leading edge
s	distance along the surface from the leading edge
S	reference wing area, ft^2
u	local velocity in boundary layer, ft/sec
u_e	velocity at boundary-layer edge, ft/sec
V	true airspeed, knots
V_c	calibrated airspeed, knots
W	airplane gross weight, lb
x	longitudinal dimension, ft
y	lateral dimension, ft
z	vertical dimension, ft
δ	boundary-layer thickness, in.
λ	wave length, in.
Λ	leading-edge sweep angle, deg
η	nondimensional semispan location, y/(b/2)

Subscripts:

$\bar{c}$	mean aerodynamic chord
ℓ	local point on airfoil
l.e.	leading edge

*Nonmember, AIAA, Aero-Space Technologist
**Member, AIAA, Aero-Space Technologist

t transition

u.s. upper surface

∞ free-stream conditions

Abbreviations:

NLF natural laminar flow

rpm revolutions per minute

Introduction

The benefits to be gained by achieving significant amounts of of natural laminar flow (NLF) on production airplanes have been inhibited by aerodynamic surface condition requirements which were too severe for early airframe structures. These surface requirements specify the allowable roughness and waviness as a function of boundary-layer characteristics. During the period in which roughness and waviness requirements for laminar flow were first developed, experience with the available riveted aluminum airframe construction techniques led to the consensus that these requirements could not be met on production airplanes. The difficulty was compounded by the relatively high Reynolds number range, $R_c > 15 \times 10^6$, for the World War II high performance fighters on which early NLF applications were attempted.

Currently, however, modern construction materials and fabrication methods offer the potential for the production of aircraft aerodynamic surfaces without significant roughness and waviness. These modern techniques include composites, milled aluminum skins and bonded aluminum skins, among others. An additional modern trend favorable to NLF is the relatively lower range of Reynolds numbers for modern NLF applications on high performance business airplanes, with typical cruise Reynolds numbers of less than 20 million and many less than 10 million (see fig. 1). This trend results from higher wing loadings and aspect ratios which produce shorter chords, and from much higher cruise altitudes for modern airplanes.

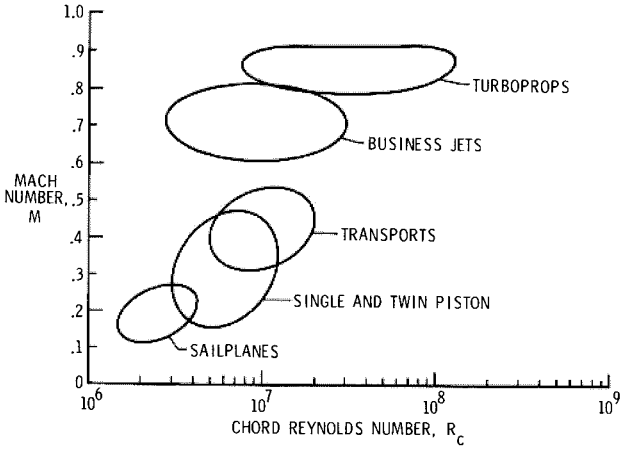

Figure 1. Representative cruise Mach and Reynolds numbers for several airplane classes.

Previous flight experiments involving NLF were limited to either airfoil gloves or specially prepared (filled and sanded) wing sections. Examples of such experiments are contained in references 1-23. On those carefully prepared surfaces, flight-measured transition locations, and hence airfoil performance, typically matched low turbulence wind-tunnel model test results very well. The previous flight experiments in which transition and/or drag were determined on unprepared (production) surfaces resulted in little or no laminar flow (for example, refs. 8 to 10, 14 to 18, and 20.)

It is significant to note that in the meantime NLF had become a practical reality for one category of aircraft - sailplanes. The achievement of laminar flow on sailplanes has been facilitated by the lower Reynolds numbers ($R_c < 4 \times 10^6$ typically (see fig. 1)) that they operate at relative to most power airplanes and by the use of composite construction methods to produce smooth complex shapes. Based on the successful NLF experience on sailplanes, the question arises as to the maximum Reynolds number range where the smoothness of modern, practical airframe construction techniques will fail to meet requirements for NLF in favorable pressure gradients.

This paper presents the results of several NLF flight experiments conducted by NASA during the past year seeking to answer this question. The significant factor distinguishing these recent flight experiments from those of the 1930's and 1940's is the difference in pre-flight preparation of the surfaces tested. The recent experiments were conducted on "production-quality" surfaces, that is, on surfaces which received (with two noted exceptions) no modification by filling and sanding to meet the airfoil contour or waviness requirements for NLF. This paper presents the major results of these flight experiments and the implications of these results for airplane design, flight test procedures, and further studies.

Flight Experiments

In the past year, NLF flight experiments[24,25] were conducted on seven different airplanes of the (seven) types listed in the table and shown in figure 2. The general objective of these flight experiments was to investigate the extent of NLF and the factors affecting transition to turbulence on a wide variety of modern, production-quality smooth airframe surfaces tested under various operating conditions. The airplanes chosen for the experiments had relatively stiff skins, free from significant roughness and waviness, and possessed relatively long runs of proverse pressure gradients, favorable to laminar boundary-layer stability. The methods of airframe construction for the test airplanes are given in the table.

Most of the surfaces evaluated for laminar flow received no special surface contour preparation prior to testing. However, in two of the tests (Cessna 210 and Learjet 28/29), the leading-edge butt joints or rivet rows were faired over to eliminate gross disturbances to the boundary layer. For the remaining six airplanes, the standard production-quality surfaces were tested. In the case of Skyrocket II, the airplane had been unprotected from the natural environment at the Charleston, West Virginia airport where it

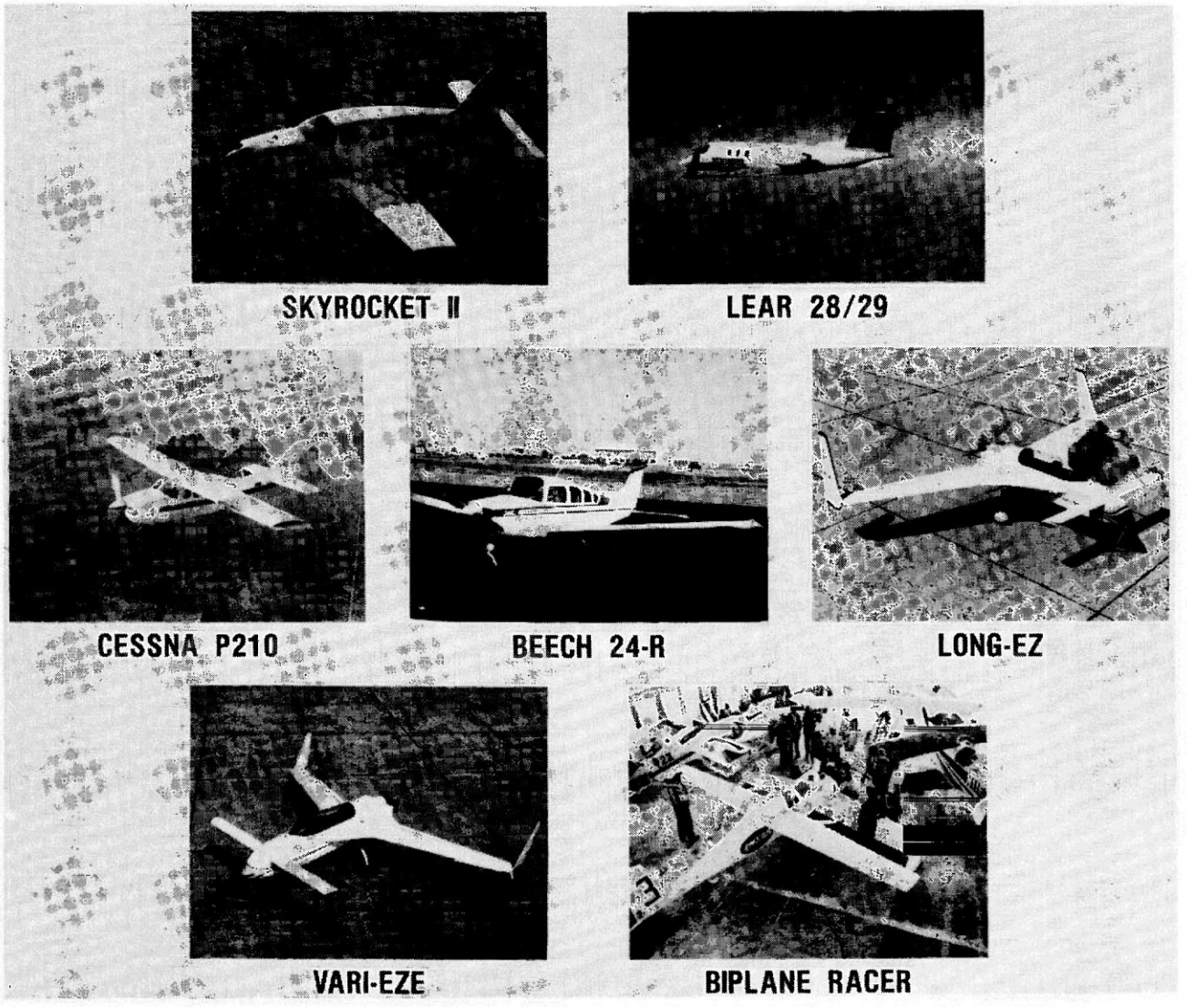

Figure 2. Airplanes selected for NLF flight experiments.

Table.- Airplanes Used in Natural Laminar Flow (NLF) Flight Experiments

Airplane	Construction	Surface	$\bar{c}$, ft	Λ, deg	Airfoil
Bellanca Skyrocket II	Fiberglass/aluminum honeycomb	Wing	5.37	3	NACA 63_2-215
Gates Learjet Model 28/29	Milled aluminum skins, integrally stiffened*	Wing	6.92	17	NACA 6-series
		Winglet	1.73	40	LS(1)-0413 mod.
Cessna P-210	Dimpled, flush-riveted aluminum**	Wing	5.08	0	NACA 64 series
Beechcraft Model 24R	Bonded aluminum skins/honeycomb ribs	Wing	0	0	63_2A-415
		Propeller	≈0.54	-	Clark Y
Rutan Long-EZ†	Fiberglass/foam core	Wing	3.13	23	Eppler
		Winglet	1.71	28	Eppler
		Canard	1.08	0	GU25-5(11)8
Rutan VariEze	Fiberglass/foam core	Wing	2.58	27	LS(1)-0417 mod.
		Winglet	1.21	29	LS(1)-0417 mod.
		Canard	1.08	0	GU25-5(11)8
Rutan Biplane Racer	Fiberglass or graphite/foam core	Fore wing	2.67	6	Eppler
		Aft wing	1.92	3	Eppler

*Leading edge to skin butt joint filled and faired smooth
**Portion of test section filled and faired smooth
†Two different Long-EZ airplanes were tested to confirm consistency of transition results

was parked outside for over 5 years. Prior to testing, the airplane was painted, but no smoothing of airfoil contours was performed. The significant point in common for all of the airplanes tested was that they possessed low levels of surface waviness and roughness which are currently achieveable in production and which appear maintainable over extended periods of airframe life.

Specific objectives of the experiments included measurements or observations of the following:

1. Boundary-layer laminar to turbulent transition locations on a variety of aerodynamic surfaces including swept and unswept wings, fuselage nose, wheel fairing, horizontal and vertical stabilizers, and propeller spinner and blade airfoil surfaces.

2. Effect of the nearly total loss of laminar flow (fixed transition at 5 percent chord) on airplane performance, stability, and control.

3. Effect of propeller slipstream on wing boundary-layer transition and on boundary-layer profiles.

4. Wing section profile drag.

5. Effect of flight through clouds on boundary-layer transition.

6. Insect debris contamination effects.

The test conditions for the experiments are shown in figure 3. Because of the variety of geometric shapes existing on each of the aircraft (tapered wings, for example) and the range of operating flight speeds and altitudes, ranges of Reynolds numbers, based on local chords, are given for individual airplane components.

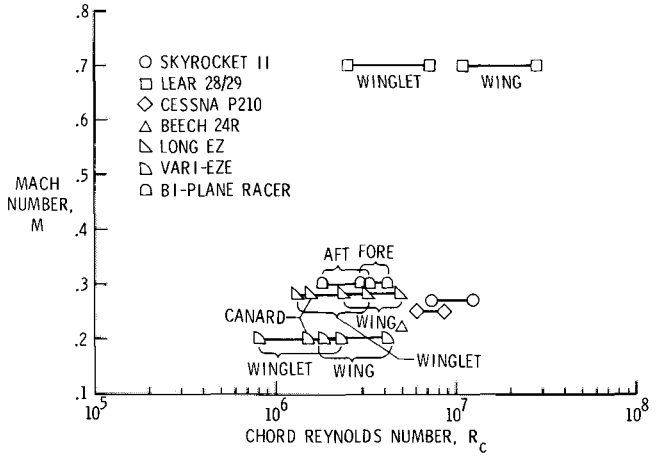

Figure 3.- Free-stream conditions for NLF flight experiments.

Experimental Methods

For all of the airplanes tested, boundary-layer transition location measurements were made using the sublimating chemical technique[26-28]. The technique involves coating the surface with a thin film of volatile chemical solid which, during exposure to free-stream airflow, rapidly sublimates in the turbulent boundary layer due to heat transfer. The chemical coating remains relatively unaffected in the laminar region because of lower heat transfer rates, thus indicating transition. The use of a chemical such as acenaphthene at ambient temperatures between 30°F and 90°F offers the capability to fly to low altitude test points (<20,000 ft), stabilize the sublimating chemical pattern at the desired test conditions, and return to the ground with the chemical pattern unaffected by the off-condition portions of the flight. The resulting range of flight times at the test conditions vary between about 60 minutes and 5 minutes, respectively for the temperatures given.

Flight measurements on the Skyrocket II airplane included wake profiles using a wake rake for section profile drag determination, boundary-layer profiles measured using boundary-layer rakes, and section-lift coefficients determined using pressure belt measurements. Speed-power data were recorded to determine relative airplane drag polar changes from free to fixed transition. For tests on the airplanes which included fixed transition, thin grit strips (1/8 in. wide) with grit sized by reference 29 were located at x/c = 5 percent on upper and lower component surfaces.

Laminar Flow Observations

Transition Locations

The location of boundary-layer transition on the lifting surfaces evaluated was observed generally to occur downstream of the analytically estimated minimum pressure locations for each airfoil at its particular flight conditions. Thus, transition is caused by amplification of 2-D Tollmein-Schlichting instabilities in the adverse pressure gradient regions or by laminar separation. The transition Reynolds numbers for the largest chords on each of the various components tested on each airplane are shown in figure 4.

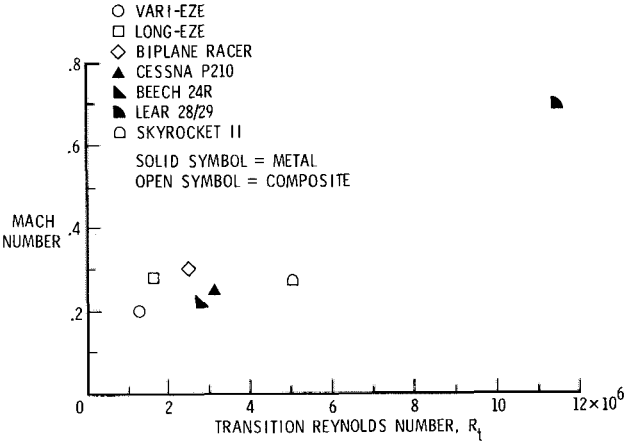

Figure 4. NLF transition Reynolds numbers from flight experiments.

Transition Reynolds numbers varied from 1 to 5 million for the propeller-driven airplanes, and exceeded 11 million for the business jet tested. Examples of boundary-layer transition visualization by sublimating chemicals are shown in figures 5 to 8.

Figure 5(a) illustrates the upper surface laminar flow transition on the Bellanca Skyrocket wing located at $(x/c)_t$ = 46 percent at the inboard wake probe station (η = 0.525) for $R_c = 9.7 \times 10^6$ and $C_\ell \approx 0.22$.

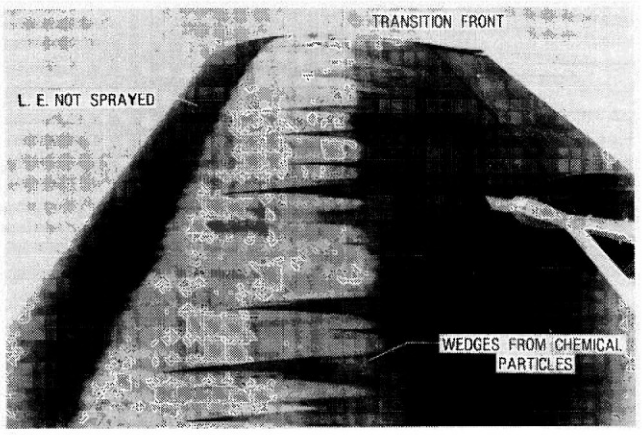

(a) Upper surface transition
Figure 5. Bellanca Skyrocket II flight data.

The turbulent wedges seen in figure 5(a) were caused by large chemical particles which adhered to the surface during application of the coating. At the same span location and test condition, the wing lower surface transition, as illustrated in figure 5(b), is located at $(x/c)_t$ = 46 percent.

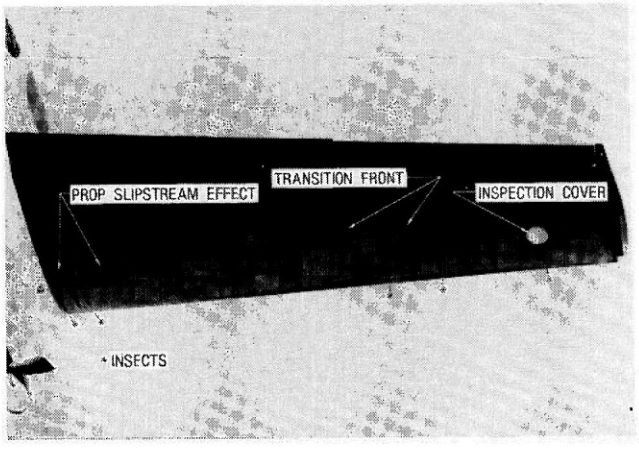

(b) Lower surface transition.
Figure 5. Continued.

Turbulent wedges caused by insects are marked with an asterisk in figure 5(c). The unmarked wedges were caused by artificial trips (grit). Note the absence of any chemical particle-induced wedges in this pattern; this resulted from mechanically loosening the particles by wiping the chemical coating with cheesecloth prior to flight. An example of a measured pressure distribution and transition locations is shown in figure 5(c). Also shown in figure 5(c) are the predicted pressure distributions and transition locations for the theoretical and actual airfoil contours on the Skyrocket wing. Fair agreement is seen between the measured and predicted characteristics for the airfoil. The theoretical airfoil calculations used NACA 63_2-215 coordinates. The actual airfoil calculations used the coordinates measured on the wing at the inboard wake probe station (η = 0.525). The measured nondimensionalized transition positions are summarized in figure 5(d).

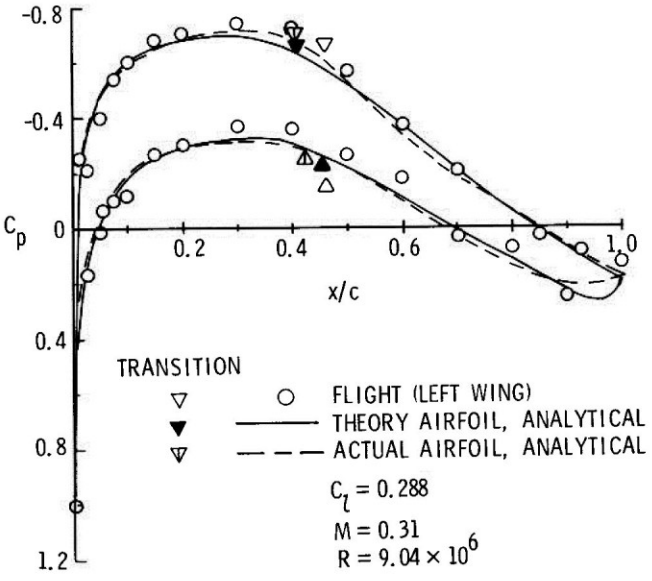

(c) Pressure distributions.
Figure 5. Continued.

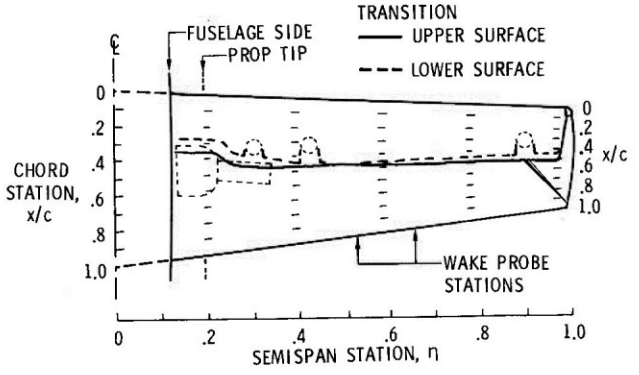

(d) Nondimensional transition locations.
Figure 5. Concluded.

Transition on the upper surface of the Learjet wing (fig. 6) was located near $(x/c)_t$ = 40 percent across the span for M = 0.7, $R_c = 21.7 \times 10^6$ and C_ℓ = 0.2. Free transition on the inboard side of the winglet was observed to occur as far back as $(x/c)_t$ = 55 percent. The unit Reynolds number during this test was $R_x = 3.08 \times 10^6$ ft^{-1}. This large value of R_x resulted from the low density altitude (16,500 ft) selected to facilitate the use of sublimating chemicals in the winter. A normal cruise unit Reynolds number for this airplane would be $R_x = 0.87 \times 10^6$ ft^{-1} for M = 0.76 at 51,000 ft cruise. Thus, the transition data from the Learjet tests were gathered at a higher Reynolds number than is required during normal operations.

Boundary-layer transition locations on the wing and strake, winglet, and canard of the Rutan Long-Ez are shown in figure 7 for

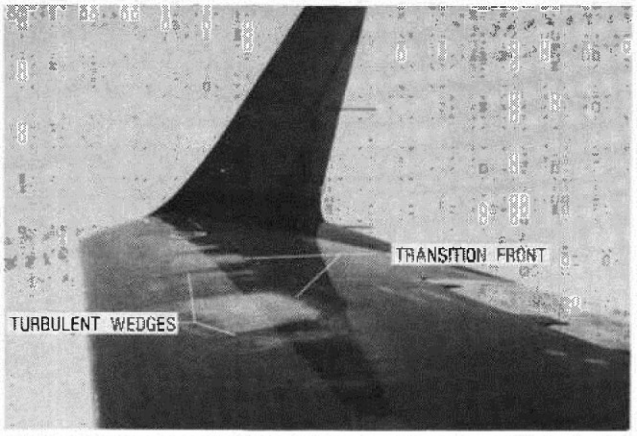

Figure 6. Gates Learjet Model 28/29 transition visualization; M = 0.7, R_x = 3.08 x 10^6 ft^{-1}, C_L = 0.12.

R_x = 1.42 x 10^6 ft^{-1} and C_L = 0.16. Wing upper surface transition is shown in figure 7(a) located at $(x/c)_t$ = 32 percent along the wing span. For the wing airfoil at the test conditions, proverse pressure gradients were estimated theoretically to exist to about $(x/c)_{u.s.}$ = 30 percent. On the strake, transition occurs (fig. 7(a)) near $(x/c)_t$ = 10-15 percent.

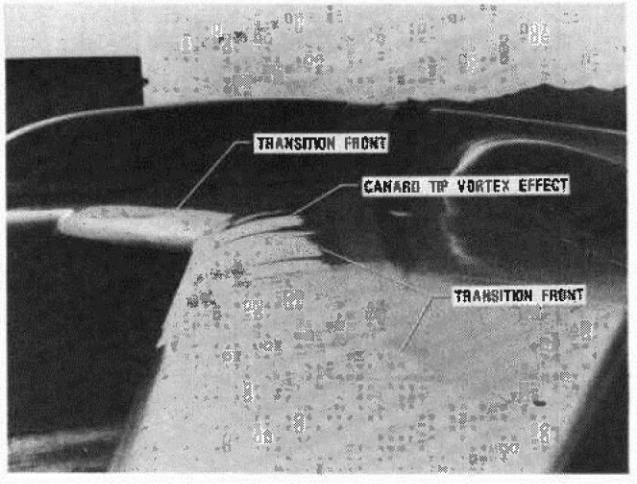

(a) Wing and strake
Figure 7. Boundary-layer transition visualization on the Rutan Long-EZ; R_x = 1.42 x 10^6 ft^{-1}, C_L = 0.16.

Transition on the winglets of this airplane (fig. 7(b)) was observed at $(x/c)_t$ = 32 percent on the inboard suction side, and on the canard upper surface (fig. 7(c)) at $(x/c)_t$ = 55 percent.

Figure 8 illustrates laminar flow on the propeller of the Beech Model 24R airplane. Boundary-layer transition was seen at $(x/c)_t$ = 38 percent on the forward (suction) side and at $(x/c)_t$ = 80 percent on the aft (pressure) side of the blade. The test was conducted at V = 133 knots, 2700 rpm, and J = 0.84. These conditions produce a local unit Reynolds number on the blade at the 50 percent blade radius location of R_x = 2.89 x 10^6 ft^{-1} and a local Mach number of 0.46.

Transition location observations on the remaining airplanes listed in Table 1, but not discussed here, were of the same nature as above.

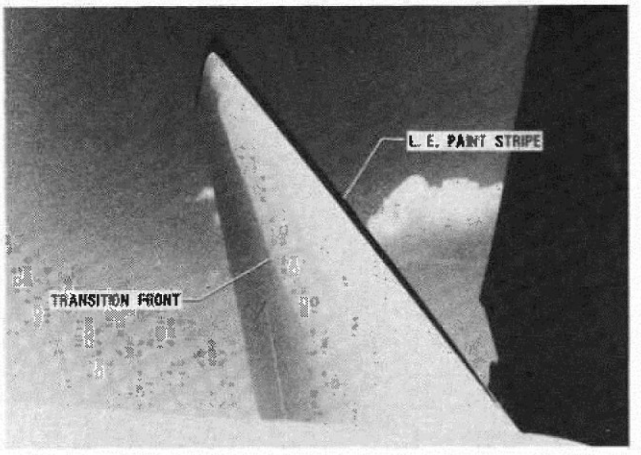

(b) Winglet
Figure 7. Continued.

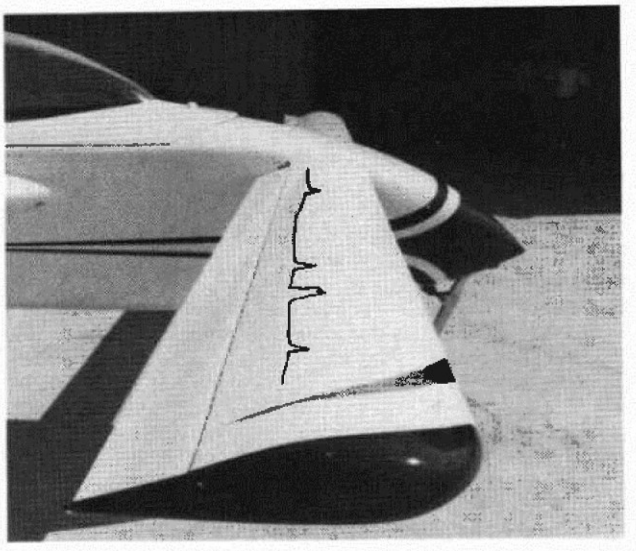

(c) Canard
Figure 7.- Concluded.

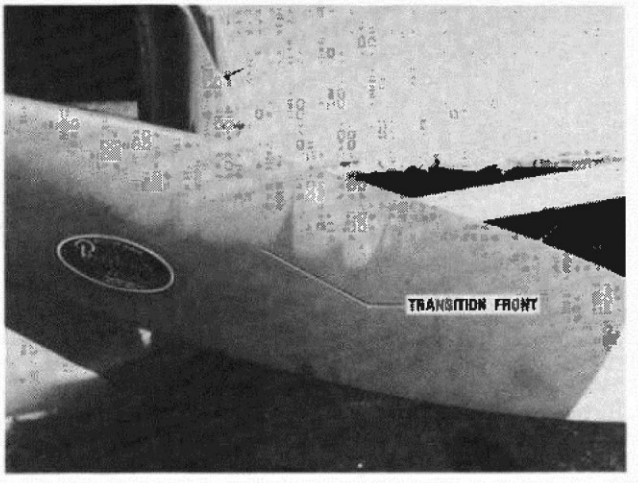

Figure 8. Boundary-layer transition visualization on a Hartzell propeller (Beech Model 24R airplane), V = 140 knots, n = 2700 rpm.

That is, laminar flow extended typically to positions slightly beyond the predicted minimum pressure point.

Surface Conditions and Contours

No premature transition was observed for any of the tests which could be attributed specifically to surface waviness. Surface waviness measurements* were made for all but two of the airplanes tested. An example of waviness is given in figure 9 for the Skyrocket II.

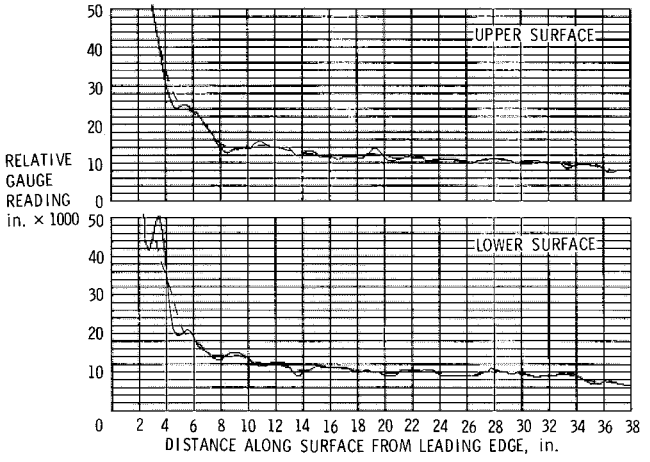

Figure 9. Indicated surface waviness for the Bellanca Skyrocket II at the inboard wake probe station.

The difference between the solid and the dashed lines serves to indicate wave height. The largest indicated wave height appears near the leading edge of the lower surface where h ≈ 0.015 in. near s = 4 in., (x/c) = 6.5 percent. This particular wave occurred at the bonded leading edge attachment joint. More typical wave heights were about h = 0.002 in.

Conservative agreement exists between allowable and actual wave heights for all of the surfaces tested, where allowable wave heights were estimated using the criterion from reference 31:

$$\frac{h}{\lambda} = \left(\frac{59{,}000\ c\ \cos^2 \Lambda}{\lambda\ R_c^{1.5}} \right)^{1/2} \qquad (1)$$

For multiple waves, h/λ is one-third the value for a single wave.

The differences between actual and allowable waviness for selected measurement locations on the airplanes tested for NLF are shown in figure 10. The allowable waviness (h/λ) is determined from equation (1) for the chord length at the largest wave found and for flight Reynolds number. As shown in the figure, for the surfaces tested, no waves existed which exceeded the empirical criterion. Also, since the testing was conducted at low altitudes and high speeds, the allowable waviness at more typical cruise conditions for each airplane will be somewhat larger.

*Surface waviness was measured with a dial indicator on a 2-in. base and is referred to as indicated waviness since the recorded values of wave amplitude and wave numbers are magnified to some extent by the measuring device[31].

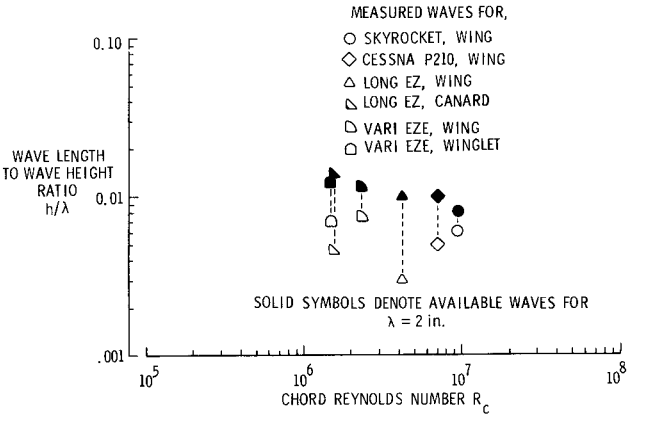

Figure 10. Comparisons of allowable and actual waviness for NLF flight experiment data.

On the Skyrocket, measurements were made of airfoil contours existing on the wing tested. Figure 11 illustrates the comparison at one wing station between theoretical NACA 63_2-215 and actual section shapes. Deviations between the actual and theoretical contours as large as 0.117 in. were measured on the upper surface. Calculations (using ref. 30) of airfoil pressure distribution and transition characteristics predict small effects for the contour deviations measured as shown in figure 5(c) by comparing the data for the theoretical and actual airfoils. The waviness and contour measurements and analyses discussed here are evidence of the ability, with modern airframe manufacturing methods, to produce surface conditions which can conservatively meet NLF roughness and waviness requirements.

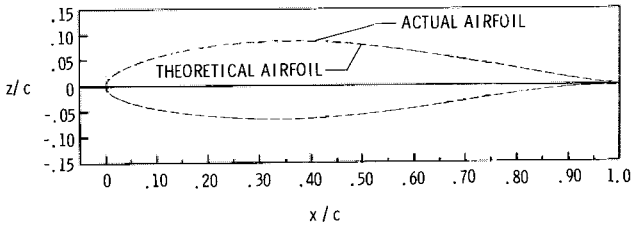

Figure 11. Comparison of the NACA 63_2-215 and actual airfoil contours for the Bellanca Skyrocket II (inboard wake probe station).

Profile Drag and Fixed Transition Effects

While the determination of transition locations is significant to the understanding of airplane performance, it is the measurement of lifting-surface profile drag, correlated with transition locations, which provides a complete understanding of airframe performance. It is also important to understand the effects on airplane aerodynamics which can occur due to the total loss of laminar flow (fixed leading-edge transition).

Flight-measured wing profile drag for the Bellanca Skyrocket II at the inboard wake probe station (see fig. 5(d)) is presented in figure 12 for free and fixed transition. This figure also presents the wind-tunnel-measured characteristics for the NACA 63_2-215 airfoil with free transition. As shown, excellent agreement exists

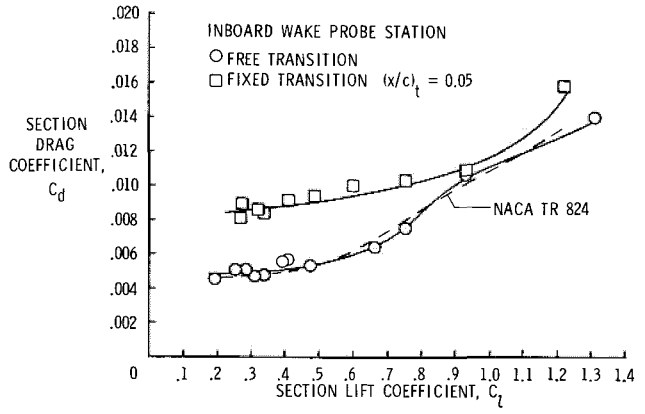

Figure 12. Comparison of flight and wind-tunnel section characteristics for the Skyrocket II airfoil (inboard wake probe station).

between the tunnel[32] and flight experiment drag polars. With fixed transition for cruise lift coefficients ($C_\ell < 0.3$), the wing section profile drag increases by 80 percent. With transition fixed on both the wing and empennage surfaces at 5 percent, total airplane drag at cruise (based on the power required at a given speed) increased 23 percent. The benefit of laminar flow on the cruise range performance of this airplane was calculated using a parabolic drag polar assumption for the airplane, airplane zero lift-drag coefficient with laminar flow of 0.0163 (from ref. 33), Oswald's airplane induced drag efficiency factor of 0.80, a constant value of brake specific fuel consumption of 0.56, and propulsive efficiency of 0.85. At the same speed, the drag reduction with laminar flow on the Skyrocket increases cruise range by 25 percent (with constant Breguet factor).

For one of the Rutan Long-EZ airplanes tested[24], the effects of fixed transition on airplane performance and longitudinal trim characteristics are presented in figure 13.

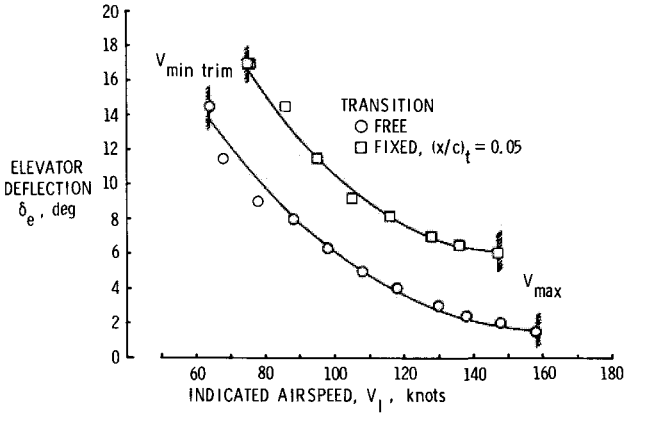

Figure 13. Comparison of fixed versus free transition performance and longitudinal control characteristics for a Rutan Long-EZ in flight.

This configuration experienced an 11 knot increase in minimum trim speed, corresponding to a 27 percent decrease in trimmed maximum lift coefficient. Maximum speed for the airplane was reduced with fixed transition by 11 knots, corresponding to a 24 percent increase in cruise drag. Figure 13 illustrates a large increase in trim elevator deflections with fixed transition on the airplane. In addition to the preceding performance degradation, qualitative observations were made of a reduction in short period damping at cruise speeds. Wind-tunnel experiments[24] confirmed that on the 20 percent thick NLF canard airfoil, fixing transition near the leading edge caused extensive separation of the thickened turbulent boundary layer near the trailing edge over the elevator. Similar large changes in performance and longitudinal stability and control were observed for one of the other airplanes tested, the Rutan VariEze[24]. The effects of fixed transition on this airplane included a reduction in trimmed airplane lift-curve slope of about 7 percent, a reduction in the lift-curve slope of the canard of about 30 percent.

Such large effects of the loss of laminar flow on the airplane aerodynamic characteristics indicate the importance of fixed transition flight testing as a standard procedure for any airplane which possesses long runs of proverse pressure gradient and smooth aerodynamic surfaces capable of supporting NLF. In addition, free transition flight testing methods should account for transition locations across all aerodynamic surfaces, using sublimating chemicals or another cost-effective technique.

Propeller Slipstream Effects

Past observations of the effect of the propeller slipstream on boundary-layer transition[4,5,14,15,32,34,35] produced varying conclusions. The research reported in references 4, 5, and 34 concluded that the effect of the slipstream was to effectively move transition to the wing leading edge behind the propeller. In the case of Young's flight experiments, boundary-layer thickness, measured by a total pressure survey probe, was used to judge transition location; where the measured boundary-layer thickness exceeded the calculated laminar thickness, transition was assumed to have occurred. Young thus reported transition near the leading edge on two different airplanes. Hood, using similar methods, reported similar results in wind-tunnel tests for a propeller mounted 20 percent chord in front of the wing leading edge. Concerns about the validity of these conclusions are discussed below.

Experiments reported in references 14, 15, and 35 gave evidence that the effect of the propeller slipstream might not be as detrimental as for Young's and Hood's tests. Wenzinger's tunnel experiments showed moderate effects of propeller slipstream on wake-probe measured section drag for an NACA 66 series NLF airfoil. Zalovcik reported extensive laminar flow in the propeller slipstream during his flight experiments on the P-47 and P-51 airplanes. These latter flight experiments were the first to rely on detailed boundary-layer rake measurements to determine transition locations as indicated by large profile changes at transition.

Two of the recent flight experiments included observations and measurements of the laminar boundary layer in the slipstream on the configurations illustrated in figure 14. On the Rutan biplane

racer[24] on the inboard portion of the aft wing immersed in the slipstream (see fig. 15), the chemical pattern in the propeller slipstream was similar to that outside the slipstream indicating transition at $(x/c)_t$ = 61 percent.

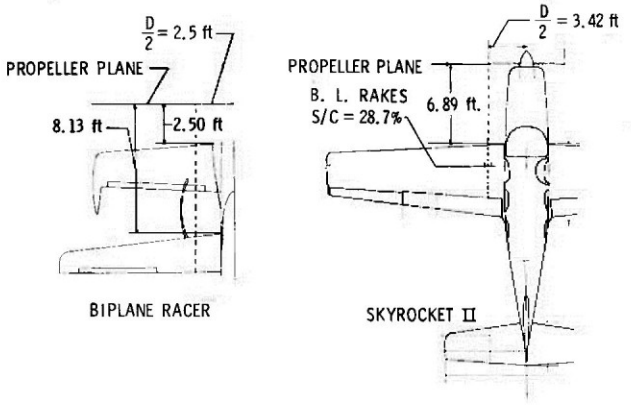

Figure 14. Planviews of configurations used to study the effects of propeller slipstream on NLF.

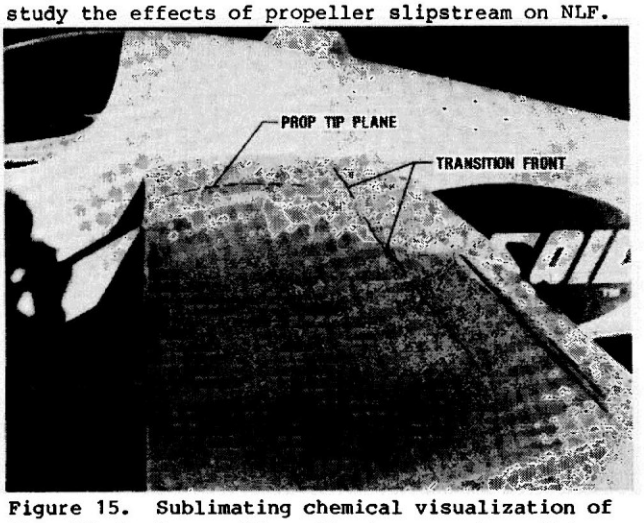

Figure 15. Sublimating chemical visualization of the effect of propeller slipstream on transition on the Rutan Biplane Racer; R_x = 1.38 x 10^6 ft^{-1}, C_L = 0.13, n = 2700 rpm.

During the Skyrocket experiments which followed, more detailed measurements were made in the propeller slipstream. Figures 5(b) and 5(d) show that transition as indicated by the chemical pattern moved forward on the upper surface from $(x/c)_t$ = 42 percent outside the slipstream to $(x/c)_t$ = 36 percent inside. On the lower surface transition moved forward by a similar increment. An interesting detail which was noted was the lack of any apparent effect of the propeller tip vortices on transition where they impinged on the wing. One possible explanation for the forward motion of chemical-indicated transition in the propeller wake is the effect of an increased disturbance environment in the propeller slipstream. These larger disturbances might amplify to transition earlier along the chord than the smaller disturbances outside the slipstream.

Time-averaged boundary-layer profiles were measured by rakes inside and outside the propeller slipstream with both free and fixed transition on the Skyrocket (see fig. 16). These measurements were made at s/c = 28.7 percent, R_x = 1.715 x 10^6 ft^{-1}, M = 0.31, and n = 1800 rpm.

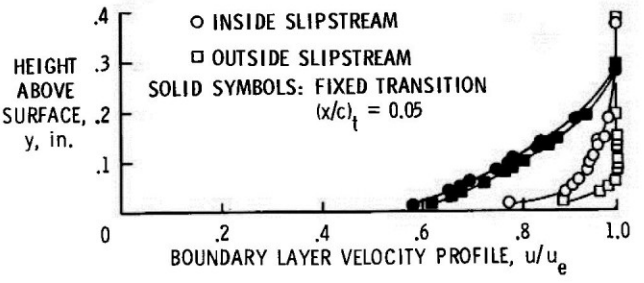

Figure 16. Effect of propeller slipstream on Skyrocket II boundary-layer profiles; s/c = 28.7 percent, n = 1800 rpm, C_L = 0.21.

Inside the slipstream the estimated unit Reynolds number was 1.778 x 10^6 ft^{-1} (using propeller momentum theory).

With free transition, figure 16 shows the thin laminar boundary layer outside the propeller slipstream where $\delta \approx 0.06$ in.; inside, the profile has thickened to $\delta \approx 0.24$ in. and the profile has changed, appearing more turbulent in shape. This rake was positioned in the slipstream at a chordwise position which was laminar as shown by sublimating chemical patterns. Thus, this thickened profile was not a turbulent one in the normal sense. To verify the shape and thickness of an actual turbulent profile at this position, transition was fixed in front of the rakes inside and outside the propeller slipstream. The resulting turbulent profiles are seen in figure 16 as the solid symbols. It is apparent that the effect of the propeller slipstream on time-averaged boundary-layer profile measurements is to create a shape which is turbulent in appearance and which is increased in thickness to near the actual turbulent boundary-layer thickness ($\delta \approx 0.28$ in. for the solid symbols).

The early measurements by both Young and Hood, using boundary-layer thickness or profile shape as an indication of transition, thus may have produced misleading conclusions about the effect of propeller slipstream on laminar flow. If this is true then there may be no data in the literature which properly conclude that propeller slipstreams cause premature transition.

A possible explanation is offered for the "turbulent-appearing" time-averaged boundary-layer profile in the laminar region of the propeller slipstream. Perhaps the cyclic impingement in the boundary layer of the propeller-blade trailing-edge vortex-sheet causes small chordwise regions of transition which move downstream in a coherent fashion. Between these turbulent "packets", the boundary layer might be "normally" laminar. In time-averaged measurements, these locally cyclic transition regions might affect the profiles as shown in figure 16.

A complete understanding of the phenomena involved in laminar boundary layers immersed in propeller slipstreams will be useful in developing methods to predict transition and possibly reduce section drag in these regions. It appears possible that some level of laminar flow drag reduction may be realized in propeller slipstreams.

Sweep Effects

The two significant wing-geometry-related phenomena which can adversely affect laminar boundary layers on swept surfaces are crossflow instability and turbulent contamination of the leading-edge attachment line flow (or leading-edge contamination). The analysis of the present NLF flight data has not yet included detailed analytical stability analysis. Since no obvious crossflow instability was observed on the swept wings and winglets in the recent flight experiments, this discussion will center on leading-edge contamination.

A comparison betweeen the recent flight data and the spanwise contamination criterion is presented in figure 17 for the VariEze and the Long-EZ[24].

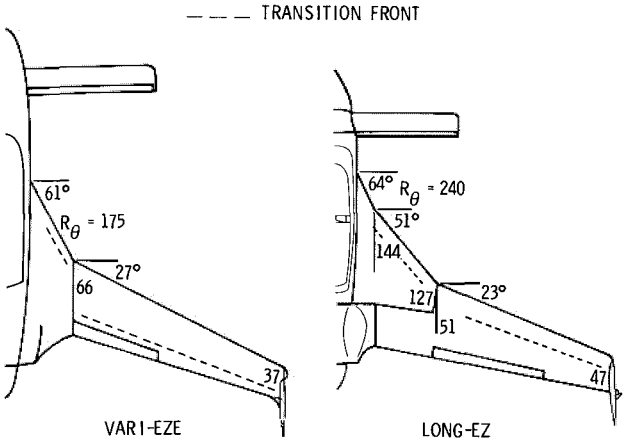

Figure 17. Comparison of NLF flight data on swept surfaces with the spanwise contamination criterion.

The spanwise contamination criterion is summarized in reference 36 as

$$R_\theta = 0.407 \frac{\sin\Lambda}{\sqrt{\cos\Lambda}} \sqrt{R_x \cdot r_{l.e.}} \qquad (2)$$

where no spanwise contamination occurs for R_θ < 100, and depending on the surface conditions (roughness), there may be no spanwise contamination for R_θ < 240. For R_θ > 240, turbulent contamination from any source will freely propagate spanwise along the attachment line. On the swept main wings for both the VariEze (Λ = 27°) and the Long-EZ (Λ = 23°), the data in figure 17 show that R_θ = 100 has not been exceeded. The same was true for the winglets on both airplanes where R_θ < 45 for the VariEze and R_θ < 36 for the Long-EZ. On the swept strakes of both the VariEze (Λ = 61°) and the Long-EZ (Λ = 51°), R_θ exceeded 100; still, small regions of laminar flow were observed near the leading edges of both strakes. Perhaps the smoothness of the leading edges permits laminar flow with R_θ > 100. Alternately, relaminarization might have been responsible for the short laminar runs observed in the strakes. On the Long-EZ, on the very short inboard strake (Λ = 64°) where $R_\theta \approx 240$, no laminar flow was recorded by the chemical pattern. At the leading-edge break between Λ = 64° and Λ = 51°, the leading-edge contamination from the 64° swept region was not observed to propagate onto the 51° swept region in spite of 148 < R_θ < 127 for this region (see fig. 17(b)).

On the Learjet wing (Λ = 17°), R_θ = 100 was not exceeded in spite of the extremely high unit Reynolds number during the test[24]. On the Learjet winglet, where R_θ varied from 151 at the root to 75 at the tip during the tests, it could not be ascertained whether spanwise contamination was present on the portions of the winglet which were turbulent. This uncertainty was due to excessive roughness in the form of screw heads which caused transition in some regions of the leading edge.

Even if spanwise contamination was present at the test condition where $R_x = 3.08 \times 10^6$ ft^{-1}, at typical cruise where $R_x = 0.87 \times 10^6$ ft^{-1}, the values of R_θ would drop to 80 at the winglet root and 40 at the tip, thus ensuring no spanwise contamination. In fact, at the Learjet cruise unit Reynolds number given above, on a surface swept 40°, the leading-edge radius could be as large as 1.5 in. and still keep R_θ < 100 for no spanwise contamination.

This observation implies that, in general, on certain relatively large lifting surfaces, spanwise contamination at high altitude cruise may not be a serious concern. On the Gulfstream American GIII airplane, for example (chosen for its large size in the business jet class), at 45,000 ft, M = 0.85 cruise, R_θ varies from 80 at the wing root to 68 at the tip, precluding spanwise contamination. As a final example of operations below the spanwise contamination criterion, R_θ for the DC-10 winglet[37] varies from 64 at the root to 40 at the tip for M = 0.82, 35,000 ft cruise. At a cruise unit Reynolds number of about 1.9×10^6 ft^{-1}, the waviness requirements for a DC-10 winglet surface appear attainable.

Based on these observations, it appears that for certain important potential applications, spanwise contamination need not be a concern for relatively large lifting surfaces. Of course, the final design of a swept NLF surface will also be strongly influenced by crossflow stability considerations.

Insect Debris Contamination

The effect of contamination of NLF wings by insect debris is an important consideration in NLF airfoil design as well as in the operation of airplanes with laminar flow wings. These considerations, as well as insect population characteristics, are discussed in some detail in the literature[38-44]. In practice, the seriousness of insect debris contamination will likely be dependent on airplane mission characteristics. On business airplanes for example, it may be reasonable to expect an airplane operator to wipe the wing leading edge clean as part of the normal walk-around pre-flight inspection. In an intensive utilization mission, as with commuter airliners for example, ground turn-around times may not allow for leading-edge cleaning between frequent landings. Also, for very large airplanes, preflight cleaning of leading edges appears impractical. In these latter cases, active methods of insect protection such as porous, fluid-exuding leading edges may serve the purposes of both insect and ice protection (see fig. 18). The ice protection performance features of such systems are discussed in reference 45, and the ability of wetted leading edges to protect against insect

debris contamination is discussed in references 46 and 47.

During the Skyrocket tests, a 2.2-hour flight was conducted at less than 500 ft above ground level at V_c = 178 knots to collect a sample insect debris contamination pattern and to distinguish by chemical sublimation between which insect strikes caused transition (supercritical) and which did not (subcritical). This flight was conducted in late March after several weeks of warm weather in the Tidewater region of Virginia between 1430 and 1630 Eastern Standard Time. Figure 19 depicts the heights and positions of the insects collected along the span of the right wing and figure 5(b) shows the lower surface insect debris contamination wedges for this flight.

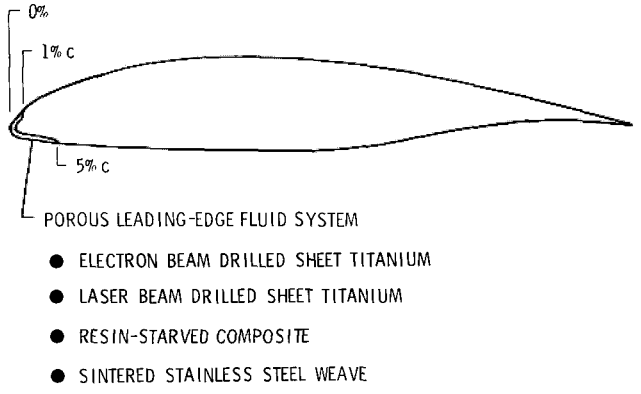

Figure 18. Ice and insect contamination protection system concept for NLF wings.

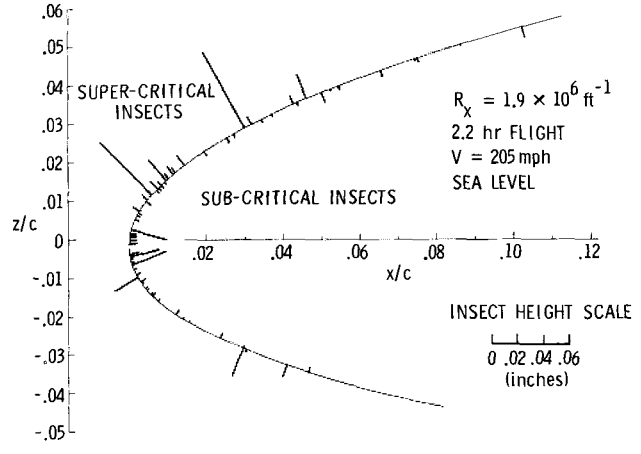

Figure 19. Insect contamination pattern on the Skyrocket II NLF wing; R_x = 1.9 x 10^6 ft^{-1}, 2.2 hour flight, V_c = 178 knots.

As illustrated by figure 19, only about one-fourth of the insects collected were of supercritical height at their chordwise locations and caused transition. Very near the stagnation point, rather large insect remains were recorded which did not cause transition. (The long duration of the flight and the relatively rapid response of the chemicals to boundary-layer turbulence - especially on the forward part of the airfoil - make it unlikely that supercritical insect strikes occurred which did not record a transition wedge in the chemical pattern.) For the 3° wing washout, the stagnation line on this leading edge varied approximately between 0 percent < (x/c) < 0.2 percent at the test conditions.

The supercritical insect strikes shown are conservative in that the unit Reynolds number during the sea level test (R_x = 1.9 x 10^6 ft^{-1}) was about 25 percent greater than a typical 25,000 ft cruise value (R_x = 1.4 x 10^6 ft^{-1}). Thus, some of the insects which were supercritical at low altitudes would become subcritical at cruise altitudes.

The sample insect contamination data presented here serve to illustrate a certain inherent level of insensitivity of this particular combination of airfoil geometry and operating conditions to insect contamination. Examples of varying sensitivity of different airfoil geometries to insect contamination effects are presented in reference 44. It is important to recognize that while sufficient insect contamination can seriously degrade airplane performance, the occurance of serious contamination levels will be infrequent for many combinations of place, time of day, time of year, airfoil geometry, and mission profiles.

Implications of Results

These recent in-flight observations of extensive regions of NLF in the favorable pressure gradient regions on several smooth, production-quality airframes have led to a new appreciation of the operational feasibility of obtaining NLF on certain modern practical airplane surfaces. The flight experiments were conducted on eight different airplanes, including both propeller- and turbojet-powered configurations and airframes constructed of aluminum or composites. The significant factor distinguishing these recent flight experiments from those of the 1930's and 1940's is the difference in pre-flight preparation of the surfaces tested. The recent experiments were conducted on surfaces which received (with noted exceptions) no contour or surface waviness modifications for NLF considerations. Transition Reynolds numbers ranged between 1 and 5 million for the propeller-driven airplanes, and exceeded 11 million for the business jet tested.

One of the objectives of the recent experiments was to determine the maximum Reynolds number range where the smoothness of modern practical airframe construction techniques will fail to meet NLF requirements in favorable pressure gradients. Based on the experimental results to date, it appears that NLF may be practical on modern production surfaces (with little sweep) for transition Reynolds numbers greater than 11 million. The absolute upper limit remains to be determined.

For several of the airplanes tested, comparisons were made between measured and allowable surface waviness. These comparisons showed, in general, that while the surfaces tested were not wave-free, the margin between actual and allowable waviness was favorable and significant.

Flight-measured wing profile drag for an NACA 63_2-215 airfoil on one of the composite airplanes tested showed excellent agreement with wind-tunnel data. The effects of fixed transition on aerodynamic characteristics of several airplanes was

measured. The results in all cases showed dramatic changes in performance and in some cases changes in stability and control characteristics. For the Bellanca Skyrocket II, cruise range is increased by 25 percent as a benefit of laminar flow. These large effects of laminar flow on airplane aerodynamic characteristics indicate the importance of conducting fixed and free transition flight testing as a standard procedure for airplanes with proverse pressure gradients on surfaces smooth enough for laminar flow. This practice holds the potential for greatly improving correlation between analysis, tunnel, and flight data.

Measurement of boundary-layer transition and profiles on the wing inside the propeller slipstream on the Skyrocket indicates extensive laminar flow in this region. The data also provides information which results in a better understanding of the effects of propeller slipstreams on laminar boundary layers. A thickened, "turbulent-appearing" boundary-layer profile was measured (in a time-averaged sense) in the laminar boundary-layer region of the wing in the propeller slipstream. These recent observations suggest that previous conclusions about the loss of laminar flow in propeller slipstreams may be incorrect, since some of the early experiments mistakenly depended on time-average-measured boundary-layer thickness or shape as an indication of transition. A possible explanation for the boundary-layer profiles observed in the propeller slipstream on the Skyrocket wing was given. The implications of these observations is that the section drag increase associated with the transition changes in propeller slipstreams may not be as large as that for fixed leading-edge transition. Thus, NLF airfoils may provide drag reduction benefits, even on multi-engine configurations with wingmounted tractor engines.

The effect of wing sweep on potential leading-edge contamination was analyzed for several of the surfaces tested in flight. The results were in general agreement with a previously established empirical criterion and no obvious leading-edge contamination was observed. The experiments conducted tended to be at higher values of unit Reynolds number relative to typical cruise values. For certain relatively large lifting surfaces, business jet wings, and transport winglets, for example, spanwise contamination at cruise may not be a significant concern. Crossflow instability is probably the principal NLF design concern for this class of swept surfaces.

Based on the recent NLF test results, maximizing the amount of laminar flow on winglets appears very promising. Past winglet applications have made frequent use of modified airfoils from the LS(1) family (formerly GA(W) family). One of the factors favoring these airfoils is their desirable maximum section lift characteristics. There are two important results from recent research which should be considered in the design of future winglet airfoil sections. The first of these recent occurences is the apparent practicality of NLF at large values of transition Reynolds number, and the second is the recent demonstration of the ability to design NLF airfoils with the same desirable values of high maximum section lift characteristics as obtained on the earlier low-speed turbulent flow airfoils[48]. In light of these two results, the design of special NLF airfoils for winglets should be considered.

The design constraints for a winglet NLF airfoil are considerably different than for a wing. On a wing, the extent of laminar flow that can be designed into the airfoil is limited by pressure recovery considerations for the fully turbulent case where separation may a problem. The same concern may not be as important for a winglet airfoil because of the relatively small effect on airplane aerodynamics due to any separation which might occasionally exist on the NLF winglet in the fully turbulent case. Thus, instead of limiting the laminar boundary-layer runs to 40 to 50 percent chord as is practical for many wing airfoils, a winglet NLF airfoil might safely support much more laminar flow. The size of the penalty for some separation in the fully turbulent case would limit the lengths of laminar runs sought. Maximum allowable pitching moment for an NLF winglet airfoil would likely be greater than for a wing since the winglet pitching-moment loads would be reacted near the horizontal plane, and therefore, with minimized weight penalty. In addition, with no control surfaces on a winglet, aft loading due to large camber is less constrained. Thus, long laminar boundary-layer runs can be sought while maintaining the flexibility in camber constraints to meet high-lift requirements.

The potential benefit of tailoring a winglet airfoil for maximum feasible laminar boundary-layer runs results from the smaller profile drag losses the winglet must overcome to produce a net gain. With sufficiently low winglet profile drag, the lift coefficient at which drag polar crossover occurs (winglets off versus on) may be outside of the flight envelope. A winglet with these characteristics would provide net performance gains throughout an airplane flight envelope.

For a sample insect debris contamination pattern collected on an NACA 6 series airfoil, only one-fourth of the insect strikes were of supercritical height, causing transition at their locations of impact. Further studies are warranted on the combinations of airfoil geometries and mission profiles which would minimize the sensitivity to serious levels of insect debris contamination. Wind-tunnel, icing tunnel, and flight experiments are planned by NASA on active systems for the protection of NLF wings against insect or ice accumulation. Such systems may be attractive for missions which allow little time between frequent landings for manual cleaning of the wing (commuter airliners, for example).

Conclusions

The following conclusions are based on the observations and measurements of boundary-layer characteristics on several modern smooth airframe surfaces:

1. The feasibility of obtaining NLF in favorable pressure gradients on certain modern practical airplane surfaces has been demonstrated for transition Reynolds numbers up to about 11 million.

2. Significant effects of laminar flow on airplane aerodynamics were measured by comparing

free- and fixed-transition test results. These large effects signify the importance of conducting fixed- and free-transition flight testing as a standard procedure for airplanes with proverse pressure gradients on surfaces smooth enough for laminar flow.

3. Significant regions of laminar flow were observed in propeller slipstreams.

4. No obvious premature transition was observed which could be attributed to excessive waviness. Conservative correlation was observed between empirically predicted allowable and actual waviness on the surfaces tested.

5. For a sample insect debris contamination pattern, only one-fourth of the insect strikes caused transition.

6. Fair correlation was observed between laminar flow observations on swept-wing leading edges and an empirical criterion for spanwise contamination.

References

[1] Stuper, J., "Investigation of Boundary Layers on an Airplane Wing in Free Flight," NACA TM 751, 1934. (Translation of "Untersuchung von Reibungsschichten am fliegenden Flugzeug," Luftfahrtforshung, Band 11, Nr. 1, vol. XI, May 1934.)

[2] Jones, M., "Flight Experiments on the Boundary Layer," Journ. Aero. Sci., vol. 5, no. 3, Jan. 1938, pp. 81-94.

[3] Stephens, A. V., and Haslam, J. A. G., "Flight Experiments on Boundary Layer Transition in Relation to Profile Drag," R&M No. 1800, Brit. A.R.C., 1938.

[4] Young, A. D., and Morris, D. E., "Note on Flight Tests on the Effect of Slipstream on Boundary Layer Flow," R&M No. 1957, Brit. A.R.C., 1939.

[5] Young, A. D., and Morris, D. E., "Further Note on Flight Tests on the Effect of Slipstream on Boundary-Layer Flow," RAE Rep. No. B.A. 1404b, 1939.

[6] Young, A. D., Serby, J. E., and Morris, D. E., "Flight Tests on the Effect of Surface Finish on Wing Drag," R&M No. 2258, Brit. A.R.C., 1932.

[7] Goett, H. J., and Bicknell, J., "Comparison of Profile Drag and Boundary-Layer Measurements Obtained in Flight and in the Full Scale Wind Tunnel," NACA TN 693, 1939.

[8] Bicknell, J., "Determination of the Profile Drag of an Airplane Wing in Flight at High Reynolds Numbers," NACA TR 667, 1939.

[9] Wetmore, J. W., Zalovcik, J. A., and Platt, R. C., "A Flight Investigation of the Boundary Layer Characteristics and Profile Drag of the NACA 35-215 Laminar Flow Airfoil at High Reynolds Numbers," NACA WR L-532, 1941.

[10] Zalovcik, J. A., "A Profile Drag Investigation In Flight on an Experimental Fighter-Type Airplane - The North American XP-51 (Air Corps. Serial No. 41-38)," NACA ACR, Nov. 1942.

[11] Tani, I., "On the Design of Airfoils in Which the Transition of the Boundary Layer is Delayed," NACA TM 1351, 1952. (Translation of "Kyo kaiso no Sen'io okuraseru Yokugata ni tuite," Rep. of the Aero. Res. Inst. Tokyo Imperial University, No. 250, vol. 19, no. 1, Jan. 1943.

[12] Zalovcik, J. A., "Profile Drag Coefficients of Conventional and Low Drag Airfoils as Obtained In Flight," NACA WR L-139, 1944.

[13] Zalovcik, J. A., Wetmore, J. W., and von Doenhoff, A. E., "Flight Investigation of Boundary Layer Control by Suction Slots on an NACA 35-215 Low Drag Airfoil at High Reynolds Numbers," NACA WR L-521, 1944.

[14] Zalovcik, J. A., and Skoog, R. B., "Flight Investigation of Boundary Layer Transition and Profile Drag of an Experimental Low-Drag Wing Installed on a Fighter-Type Airplane," NACA WR L-94, 1945.

[15] Zalovcik, J. A., "Flight Investigation of the Boundary Layer and Profile Drag Characteristics of Smooth Wing Sections on a P-47D Airplane," NACA WR L-86, 1945.

[16] Zalovcik, J. A., and Daum, F. L., "Flight Investigation at High Speeds of Profile Drag of Wing of a P-47D Airplane Having Production Surfaces Covered With Camouflage Paint," NACA WR L-98, 1946.

[17] Plascott, R. H., "Profile Drag Measurements on Hurricane II Z.3687 Fitted With "Low-Drag" Section Wings. RAE Rep. No. AERO 2153, 1946.

[18] Plascott, R. H., Higton, D. J., and Smith, F., "Flight Tests on Hurricane II Z.3687 Fitted With Special Wing of Low Drag Design," R&M No. 2546, Brit. A.R.C., 1946.

[19] Smith, F., and Higton, D. J., "Flight Tests on A King Cobra FZ 440 to Investigate the Practical Requirements for the Achievement of Low Profile Drag Coefficients on a "Low Drag" Aerofoil. R&M No. 2375, Brit. A.R.C., 1950.

[20] Britland, C. M., "Determination of the Position of Boundary-Layer Transition on a Specially Prepared Section of Wing in Flight at Moderate Reynolds Number and Mach Number," RAE TM AERO 193, 1951.

[21] Davies, H., "Some Aspects of Flight Research," Journ. of Roy. Aero. Soc., June 1951.

[22] Gray, W. E., and Davies, H., "Note on the Maintenance of Laminar Flow Wings," R&M No. 2485, Brit. A.R.C., 1952.

[23] Montoya, L. C., Steers, L. L., Christopher, D., and Trujillo, B., "Natural Laminar Flow Glove Flight Results," NASA CP-2208, 1981, pp. 11-20.

[24]Holmes, B. J., Yip, L. P., Coy, P. F., and Obara, C. J., "Flight and Wind-Tunnel Investigations of Natural Laminar Flow on Modern Airplane Surfaces," NASA TP to be published, 1982.

[25]Holmes, B. J., Hoffman, M. J., Obara, C. J., and Gregorek, G. M., "Natural Laminar Boundary Layer Flight Test Data on a High Performance Single-Propeller-Driven Composite Airplane," NASA TP to be published, 1982.

[26]Pringle, G. E., and Main-Smith, J. D., "Boundary Layer Transition Indicated by Sublimation," RAE Tech. Note AERO No. 1652 (ARC 8892), 1945.

[27]Main-Smith, J. D., "Chemical Solids as Diffusible Coating Films for Visual Indication of Boundary Layer Transition in Air and Water," R&M No. 2755, Brit. A.R.C., 1950.

[28]Owen, P. R., and Ormerod, A. O., "Evaporation From the Surface of a Body in an Airstream," R&M No. 2875, Brit. A.R.C., 1951.

[29]Braslow, A. L., and Knox, E. C., "Simplified Method for Determination of Critical Height of Distributed Roughness Particles for Boundary Layer Transition at Mach Numbers From 0 to 5," NACA TN 4363, 1958.

[30]Stevens, W. A., Goradia, S. H., and Braden, J. A., "Mathematical Model for Two-Dimensional Multi-Component Airfoils in Viscous Flow," NASA CR-1843, 1971.

[31]Anon, "Final Report on LFC Aircraft Design Data Laminar Flow Control Demonstration Program," NOR 67-136 (Contract AF33(657)-13930), Northrop Corp., June 1967. (Available from DDC as AD 819 317.)

[32]Abbott, I. H., von Doenhoff, A. E., and Stivers, L. S., Jr., "Sumamry of Airfoil Data," NACA TR-824, 1945.

[33]Gregorek, G. M., Hoffman, M. J., Payne, H., and Harris, J. P., "Drag Evaluation of the Bellanca Skyrocket II," SAE Paper No. 770472, 1977.

[34]Hood, M. J., and Gaydos, M. E., "Effects of Propellers and Vibration on the Extent of Laminar Flow on the NACA 27-212 Airfoil," NACA ACR (WR L-784), 1939.

[35]Wenzinger, C. J., "Wind Tunnel Investigation of Several Factors Affecting the Performance of a High Speed Pursuit Airplane with Air-Cooled Engine," NACA ACR, Nov. 1941.

[36]Beasley, J. A., "Calculation of the Laminar Boundary Layer and Prediction of Transition on a Sheared Wing," R&M No. 3787, Brit. A.R.C., 1976.

[37]Gilkey, R. D., "Design and Wind Tunnel Tests of Winglets on a DC-10 Wing," NASA CR-3119, 1979.

[38]Glick, P. A., "The Distribution of Insects, Spiders and Mites in the Air," U.S. Dept. of Agriculture Tech. Bull. No. 673, 1939.

[39]Freeman, J. A., "Studies in the Distribution of Insects by Aerial Currents. The Insect Population in the Air From Ground Level to 300 Feet," J. An. Ecol., 14, 128-154, 1945.

[40]Atkins, P. B., "Wing Leading Edge Contamination by Insects. ARL (Australia) Flight Note No. 17, Oct. 1951.

[41]Johnson, D., "Brief Measurements of Insect Contamination on Aircraft Wings. Aero. Res. Council TR 14999, May 1952.

[42]Lachmann, G. V., "Aspects of Insect Contamination in Relation to Laminar Flow Aircraft," C.P. No. 484, HMSO, London, 1960.

[43]Coleman, W. S., "Roughness Due to Insects. Boundary Layer and Flow Control-Its Principles and Application, Vol. 2," Pergamon Press, 1961.

[44]Boermanns, L. M. M., and Selen, H. J. W., "On the Design of Some Airfoils for Sailplane Application," Delf University of Technology, Department of Aerospace Engineering, April 1981.

[45]Kohlman, D. L., "Icing Tunnel Tests of a Glycol-Exuding Porous Leading Edge Ice Protection System on a General Aviation Airfoil," NASA CR-165444, 1981.

[46]Lockheed-Georgia Co., "Evaluation of Laminar Flow Control System Concepts for Subsonic Commercial Transport Aircraft," NASA CR-159253, 1980.

[47]Peterson, J. B., Jr., and Fisher, D. F., "Flight Investigation of Insect Contamination and Its Alleviation," NASA CP-2036, 1978, pp. 357-374.

[48]Somers, D. M., "Design and Experimental Results for a Natural Laminar Flow Airfoil for General Aviation Applications," NASA TP 1861, 1981.